COMPACT FFAG ACCELERATORS FOR MEDIUM ENERGY HADRON APPLICATIONS*

B. Qin†, Y. Ishi, Y. Mori, Y. Kuriyama, T. Uesugi
Kyoto University Research Reactor Institute, Osaka, Japan
K. Okabe, Fukui University, Fukui, Japan
JB. Lagrange, T. Planche‡, E. Yamakawa
Graduate School of Engineering, Kyoto University, Kyoto, Japan

Abstract

Medium energy hadron beams are widely applied in proton sources for generation of intense secondary beams, and medical accelerators for carbon therapy. Spiral scaling FFAG can be used for these purposes due to its compactness. Two designs using spiral FFAG rings that aims at ADSR (accelerator driven subcritical reactors) and carbon therapy are introduced.

INTRODUCTION

Medium energy hadron beams (kinetic energy around 1.0GeV proton), have important applications in proton drivers for intense neutrons / muons beam and carbon therapy. Existing candidate machines are synchrotrons, superconducting cyclotrons, linacs and FFAGs. The characteristics of strong focusing and zero chromaticity in scaling FFAGs make them attractive in various applications [1]. Furthermore, a small magnet aperture size with high field index and fast acceleration with fixed field renders this type of accelerator competitive versus synchrotrons and cyclotrons in the area of medium energy hadron beam applications.

This paper introduced two applications using spiral scaling FFAGs: 1) A 700MeV proton ring for ADSR application; 2) a 400MeV/u carbon ring for hadron therapy, which uses a novel super-ferric scheme.

LATTICE CONSIDERATIONS

Spiral sector scaling FFAG is chosen due to smaller circumference factor. By using a careful design of the magnet, the vertical tune shift can be minimized even larger difference of the pole gap size exists. The lattice parameters constraints lies on: 1) Small radius excursion for specific momentum ratio; 2) The operational betatron tunes should be far away from low-order normal structural resonances; 3) For practical factor, a reasonable spiral angle ($\zeta < 60°$) and enough space for installation of RF cavities and kicker / septum magnets should be used.

The radius excursion is determined by Eq. 1. A higher field index k is preferred to make a compact magnet sector. However, the spiral angle and horizontal phase advance limit the choice of k.

$$\Delta r = ((p_{ext}/p_{inj})^{\frac{1}{1+k}} - 1) \cdot r_0 \qquad (1)$$

Parameters Search

The linear matrix method can be used for determination of the cell number N and approximate range of k. Since transverse beam acceptances are important criterion especially for high intensity beam applications such as ADSR, more sophisticated ray-tracing code like Zgoubi [2] is required. The soft edge model with enge coefficients fitted to the TOSCA [3] model can be used for fast scan of working points and corresponding transverse acceptances.

Semi-scaling Field with Variable Spiral Angle in Spiral FFAG Sectors

The sufficient condition of zero chromaticity in scaling FFAGs requires perfect scaling magnetic field:

$$B_z(r, \theta) = B_0 \cdot (r/r_0)^k \cdot \mathcal{F}(\theta) \qquad (2)$$

where k is the constant local geometrical field index independent of the azimuthal position θ, and $\mathcal{F}(\theta)$ is the azimuthal field distribution function independent of the radius r, but has a shift equal to $\tan\zeta \cdot \ln(r/r_0)$ in spiral sectors. However, in realistic magnets adopting variable pole gaps, the fringe field will change along the radius thus breaks the scaling condition. Fortunately Eq. 2 is not the necessary condition. In linear thin lens approximation, the transverse tunes can be obtained from the transfer matrix of the spiral sector [4]:

$$\nu_x^2 \approx 1 + k\ , \quad \nu_z^2 \approx -k + F \cdot (1 + 2\tan^2\zeta) \qquad (3)$$

Obviously k should be kept constant to keep ν_x unchanged. For field flutter F, there exists difference in variable pole gaps especially for high field magnets, that causes a tune shift $\Delta\nu_z$. To make compensation, a minute change of the local spiral angle $-\Delta\zeta$ can be estimated from Eq. 4.

$$\frac{d\nu_z}{d\zeta} = \frac{2F \cdot \tan\zeta}{\sqrt{-k + F(1 + 2\tan^2\zeta)} \cdot \cos^2\zeta} \qquad (4)$$

This method was proved to be effetive by TOSCA simulation in high field FFAG magnets [5], and the chromaticity can be minimized by employing this 'semi-scaling' magnetic field.

* Work supported by Japan Science and Technology Agency
† bin-qin@rri.kyoto-u.ac.jp
‡ Moved to TRIUMF, Canada

700 MEV PROTON RING FOR ADSR

In ADSR system, the spallation neutrons produced at the target is related to beam energy and intensity delivered by the proton driver. 0.2-1.0 GeV is a good energy region, and for 700MeV proton beam, the neutron multiplication rate per proton is about 10. Here we give a design example of 700MeV proton FFAG ring.

The lattice parameters are scanned by linear matrix method and ray-tracing enge model, then finally validated using TOSCA simulated field maps. Figure 1 shows the parameters search for cell number $N = 14$. The working points with black-edge are calculated using Zgoubi FFAG-SPI routine [2] with fitted Enge coefficients. The area of the working point is scaled to the horizontal acceptance, and darker color means larger vertical acceptance. The red-edge points are samples calculated from TOSCA models. Normal sextupoles / octupoles resonances and the value of k have significant influence on transverse acceptances. Working point A was selected for this proton ring, with acceptance $\epsilon_x = 12000 / \epsilon_z = 450\,(\pi\,mm \cdot mrad)$. The parameters are listed in Table 1. The injector of this ring could be a linac. To obtain high intensity pulse beam and avoid significant tune shift due to space charge, 1kHz repetition rate is desired for 1MW beam power.

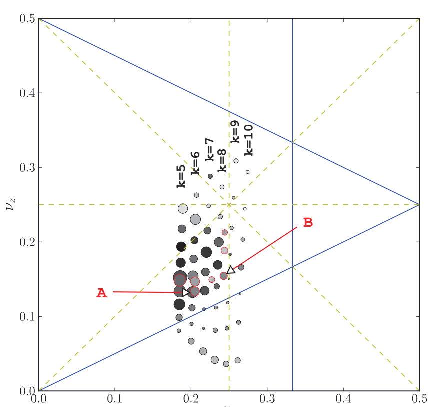

Figure 1: Parameters search for cell tune and corresponding transverse acceptances.

During the magnet design procedures, field clamps and variable pole chamfer are used to limit the fringe field and decrease the change of field flutter along radius. Iterative corrections on the pole gap and field boundary are performed to control the transverse tune shift of the 14 cells ring within 0.1, that avoids lower order resonance crossing. The tune variation is shown in Fig. 2, and detailed magnet design was described in [6]. Beam transmission is investigated for initial emmitance $\epsilon_x = 800 / \epsilon_z = 200\,(\pi\,mm \cdot mrad)$ with water-bag distribution, and the beam loss rate is less than 5% for 200 turns after injection, with 200 keV/turn acceleration speed.

The 700MeV upgrade ring plan for FFAG complex in

Table 1: Parameters of the 700 MeV Ring

Cell number	14
Injection / Extraction energy	150 / 700 MeV
Field index	6.2
Spiral angle	58.0 degree
Packing factor	0.36
Average orbit radius	6.85-7.75 m
B_{max} @ extraction	1.45T
ν_x/ν_z per cell	0.20 / 0.13
β_x/β_z @ inj.	1.6 - 4.0m / 2.9 - 6.5m
Dispersion @ inj.	0.3 - 0.85 m

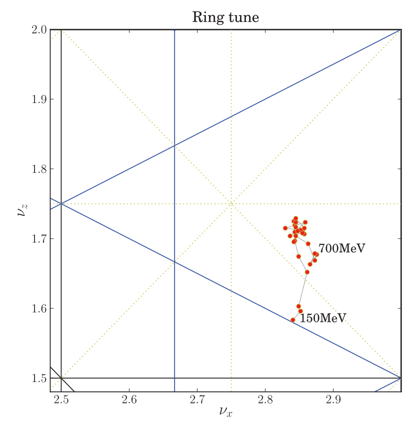

Figure 2: Variation of the ring tune

KURRI is under consideration as well [7]. Since the injection radius should be larger than 8m to match the present main ring, a higher k is preferred to keep compact radius excursion. Working point B in Fig. 1 can be chosen with $k = 8.4$, $\zeta = 58.5°$, $\epsilon_x = 8000 / \epsilon_z = 400\,(\pi\,mm \cdot mrad)$

400MEV/U C^{6+} RING FOR CARBON THERAPY

Recently, carbon therapy has been transformed from research oriented to clinically oriented. Four carbon therapy centers have been established in Japan and German, and some new designs including scaling and non-scaling FFAGs have been proposed [8]. Present medical centers for carbon therapy all employs synchrotrons with diameters larger than 20 m. However, it is possible to construct a more compact ring by using high field super-ferric FFAGs. Figure 3 is our proposed layout of a compact carbon ring, which is composed of one main spiral FFAG ring, with an IH linac injector. Main parameters are listed in Table 2.

Design study of this carbon ring was described in [5]. The main features are:

- Since it's difficult to achieve $k \approx 4$ by iron pole due to its saturation at high field, exotic rare-earth metal such as holmium (Ho) or gadolinium(Gd) are considered

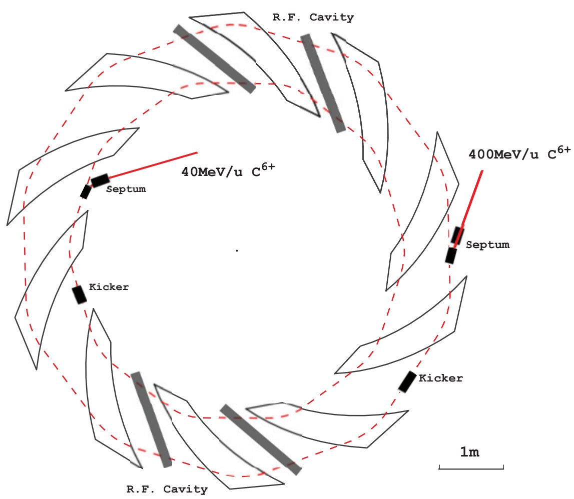

Figure 3: Schematic plan of the spiral FFAG ring for carbon therapy

Table 2: Parameters of the Carbon FFAG Ring

Parameter	Value
Particle species	$^{12}C^{6+}$
Cell number	10
Injection/extraction energy	40 MeV/u, 400MeV/u
Momentum ratio	3.45
Field index	3.6
Spiral angle	51.0°
Packing factor	0.35
ν_x/ν_z per cell	0.24 / 0.18
β_x/β_z @ inj.	0.7 - 2.3m / 0.9 - 2.6m
Dispersion @ inj.	0.2 - 0.7 m
Average orbit radius	2.6-3.45 m
Ring diameter	9m
B_{max} @ extraction	5.3T
Total current of coil	350 kA-T

for their higher permeability [9].

- The high field spiral FFAG magnet is demonstrated in Fig. 4. Multi-layer pole combining Ho and iron is used to achieve high gradient. The BH data of Ho for simulation is taken from ref. [10]. Since the magnetic reluctance in Ho and saturated iron is much larger than one in un-saturated iron part, the layer height need be modulated to keep balance of reluctance in the air gap. The coil position is important because magnetic field H becomes a dominant part in the total induction field.
- The field flutter F has a large difference between injection and extraction radii, thus causes significant vertical tune shift even after corrections on k and field boundary. The minute modification on the spiral angle is required, as shown in Fig. 5.

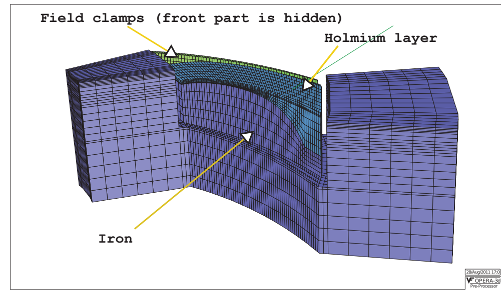

Figure 4: TOSCA model of multi-layer superferric magnet. (clamp in front and coils are hidden)

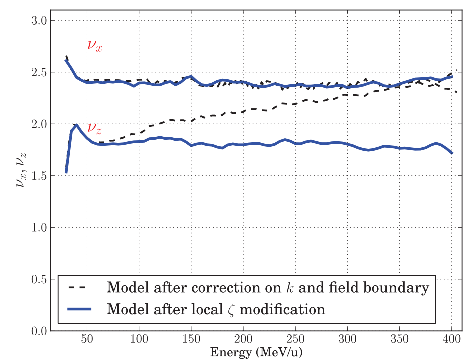

Figure 5: Minimization of tune shift in the ring during optimization procedures.

DISCUSSION

Intensive study on FFAGs for medium energy hadron beam with some applications has been performed. For carbon therapy purpose, another arrangement is to split one main ring into two rings. The first ring covers energy from 5MeV/u to 65MeV/u, can be used for proton therapy (20MeV to 240MeV) as well; the second ring covers energy from 65MeV/u to 400MeV/u. Meantime the injection energy is moderate for the linac injector.

REFERENCES

[1] Y. Mori, Nucl. Instr. Meth. A, 563(2006) 591-595.

[2] J. Fourrier et al., Nucl. Instr. Meth. A, 589 (2008) 133-142.

[3] Opera-3D User Guide,Vector Fields Limited, England.

[4] R. Baartman, Isochronous and Scaling FFAGs, AIP Conf. Proc., 642:200-203, 2003.

[5] B. Qin, Y. Mori, Nucl. Instr. Meth. A, 648 (2011) 28-34

[6] B. Qin et al., Design of high energy hadron FFAGs for ADSR and other applications, CYCLOTRON 10, Lanzhou, 2010.

[7] Y. Ishi, et al., Present status and future of FFAGs at KURRI and the first ADSR experiment, Proc. of IPAC10, Kyoto, 2010. p. 1323.

[8] U. Amaldi et al., Nucl. Instr. Meth. A, 620(2010) 563-577.

[9] D.B. Barlow et al., Nucl. Instr. Meth. A, 313(1992) 311-314

[10] W. Schauer and F. Arendt, Cryogenics, 23 (1983) 562.